

# Magnetic oscillations and field induced spin density waves in (TMTSF)<sub>2</sub>ClO<sub>4</sub>

Danko Radić, Aleksa Bjeliš

*Department of Physics, Faculty of Science, University of Zagreb, POB 162, 10001 Zagreb, Croatia*

Dražen Zanchi

*Laboratoire de Physique Théorique et Hautes Energies, Paris, France.*

We report an analysis of the effects of magnetic field on a quasi-one-dimensional band of interacting electrons with a transverse dimerizing potential. One-particle problem in bond-antibond representation is solved exactly. The resulting propagator is used to calculate the spin-density-wave (SDW) response of the interacting system within the matrix RPA for the SDW susceptibility. We predict the magnetic field induced transition of the first order between interband SDW<sub>0</sub> and intra-band SDW<sub>±</sub> phases. We reproduce the rapid oscillations with a period of 260 Tesla and the overall profile of the TMTSF<sub>2</sub>ClO<sub>4</sub> phase diagram.

PACS numbers: 71.10.Hf, 72.20.My, 74.70.Kn

Investigations of quasi-one-dimensional electronic systems at high magnetic fields and at low temperatures continue to give an important insight into the one-particle properties and interaction-induced phases such as spin- and charge-density-wave, superconductivity, and Mott localization. [1] One of most spectacular phases of this kind are field-induced spin density wave (FISDW), found in Bechgaard salts [2] and in some other low-dimensional compounds.[3] The phenomenon of the FISDW is well understood in the Bechgaard salt (TMTSF)<sub>2</sub>PF<sub>6</sub> where the cascade of SDW phases with quantized wave-vector is induced by orbital effects of magnetic field to the quasi-one-dimensional orbits of band electrons. Theory based on the mechanism of quantized nesting [4] reproduces satisfactorily main experimental data for this salt.

In this letter we concentrate on (TMTSF)<sub>2</sub>ClO<sub>4</sub>, a Bechgaard salt which after a slow cooling [5, 6] enters into a qualitatively different type of FISDW phase at low temperatures, with a phase diagram that is still, after more than ten years of intensive studies [1, 2], a matter of both experimental and theoretic controversies. In particular for magnetic field  $B > 8\text{T}$  the nature of the ordering in the relaxed material is not a simple FISDW with some low integer quantum number  $N$ , but a qualitatively different state containing several puzzling subphases.[2, 7, 8] This phase is at 8T separated by a line of first order transition from a cascade of FISDW phases which very much resembles to that of the standard model. Another characteristic phenomenon, the rapid oscillations (RO) in  $1/B$  with a frequency of 260 Tesla are visible in transport properties in both metallic *and* FISDW state.[2, 8, 9] Similar RO are seen also in thermodynamic quantities like torque, magnetization, sound velocity and specific heat, but only in the ordered phase.[1, 2] The highest value of  $T_c$  in the  $T_c(B)$  dependence is 5.5K, instead of 12K as expected from analogy with the (TMTSF)<sub>2</sub>PF<sub>6</sub> salt.

The incompatibility of above facts with the quan-

tum nesting model (QNM) for a single quasi-1D band is believed to stem from the particular ordering of ClO<sub>4</sub> anions.[2] This ordering introduces the new modulation with the wave vector  $(0, \pi/b, 0)$ , i. e. a dimerization in the low-conducting direction with the inter-chain distance  $b$ . The magnitude of the dimerizing potential can be tuned to some extent by varying the cooling rate [5, 6]. Thus, anions presumably remain disordered in the rapidly quenched samples. Then there is no dimerization gap in the band, and the system shows properties of a *single* quasi-1D imperfectly nested band with a SDW order appearing already in the zero magnetic field [5, 6, 10]. The anion ordering in slowly relaxed samples is at about 24K, and coincides with the onset of rapid oscillations in the magnetoresistance.[11]

The dimerized band has two pairs of Fermi sheets in the new Brillouin zone. Already simple geometric arguments [7] suggest three possible nesting wave vectors favoring various SDW phases. First, interband nesting, leads to SDW<sub>0</sub> that is the two-band version of the standard FISDW phase. Other two nesting vectors relate Fermi sheets within the same band. They give SDW<sub>+</sub> for antibond nesting and SDW<sub>-</sub> for bond nesting. However the interplay between SDW<sub>0</sub> and SDW<sub>±</sub> is not only a geometric question of the choice of the nesting vector. Due to a finite anion potential  $V$  in the kinetic part of the Hamiltonian an off-diagonal term appears in the SDW response, making necessary an appropriate matrix approach [12, 13] in the calculation of the critical susceptibilities. The response matrix is formulated in the space of two order parameters,  $\Delta_h$  (“homogeneous”) and  $\Delta_a$  (“alternating”), determining the magnetic pattern

$$m_z(x, R_\perp) = (\Delta_h \pm \Delta_a) \cos[(2k_F + k)x + pnd]. \quad (1)$$

Here  $d \equiv 2b$  and the upper and lower sign stay for even ( $R_\perp = nd$ ) and odd ( $R_\perp = nd + d/2$ ) chains respectively. As it is shown in Refs. [12, 13], SDW<sub>0</sub> [ $\Delta_h \neq 0, \Delta_a = 0$ ] is stabilized for low values of  $V$  (providing the imperfect

nesting parameter  $t'_b$  allows for SDW stabilization), while SDW $_{\pm}$  with  $\Delta_h \geq \Delta_a \neq 0$  gets stable for  $V/t_b > 1.6$  irrespectively to the value of  $t'_b$ . Here  $t_b$  is the interchain hopping integral. The slowly relaxed (TMTSF) $_2$ ClO $_4$  samples are expected to lie in the range of intermediate values of  $V$  in which there is no SDW ordering at  $B = 0$  down to  $T = 0$ .

Indeed, as it will be shown,  $V/t_b$  fitting the experiments is close to one. In this range it is not allowed to use the quasi-classical approximation of Gor'kov and Lebed [16], which consists in making Peierls substitution  $p \rightarrow p - eA$  in each sub-band separately and including the anions' effects only via magnetic breakdown (MB) junctions near the zone boundary. While this approximation is sufficient for  $V/t_b \ll 1$ , here one has to solve the whole quantum-mechanical problem instead.

It was pointed out several times (see [8] and references therein) that a mechanism of coherent inter-band tunnelling, very similar to Stark over-gap quantum interference (QI) in magnesium [14], is essential for high-field physics in (TMTSF) $_2$ ClO $_4$ . In particular, RO in metallic state can be explained only in terms of QI mechanism because no closed orbits exist. On the contrary, in the SDW state both closed orbits *and* Stark interference contribute to RO. Oscillating behavior periodic in  $1/B$  can be seen already at the level of one-particle spectrum. Namely, electronic propagator with longitudinal momentum  $k$  has poles at

$$E_f = v_F [f(k - k_F) + GN] \pm v_F G \delta, \quad (2)$$

where  $f$  is left-right index,  $G \equiv eBb/\hbar$  is the magnetic wavenumber and  $N$  is integer number. The first term in eq.(2) is the standard QNM dispersion and the last term is the splitting due to anions. Over-gap resonances are present in  $\delta(B)$  as will be discussed below (see Fig.1). The expression for the spectrum (2) is common to perturbation calculations [15], to quasi-classical tunnelling analysis [16], and to our exact solution as well. What changes from one approach to another are the dependence  $\delta(B)$  and the result for electronic wavefunction. In order to obtain them exactly we start from the effective one-particle Hamiltonian for electronic operators  $\Psi_f(x, p)$

$$H_0 = iv_F \rho_3 \partial_x + \tau_3 \mathcal{T}(pb - Gx) + \tilde{\mathcal{T}}(pb - Gx) - V \tau_1, \quad (3)$$

where  $\rho$ 's and  $\tau$ 's are Pauli matrices in left-right and bond-antibond indices respectively. The most general transverse dispersion was split into two parts

$$\mathcal{T}(pb) \equiv 2 \sum_{j=1}^{\infty} t_j \cos[(2j-1)pb], \quad \tilde{\mathcal{T}}(pb) \equiv 2 \sum_{j=1}^{\infty} t'_j \cos[2jpb] \quad (4)$$

corresponding to effective hoppings [17] between odd and even neighbors respectively. We diagonalize  $H_0$  by the

unitary transform

$$\Psi_f = \begin{pmatrix} \alpha_f & \beta_f \\ -\beta_f^* & \alpha_f^* \end{pmatrix} e^{if\theta} \Phi_f, \quad (5)$$

with  $|\alpha|^2 + |\beta|^2 = 1$ , and functions  $\alpha$ ,  $\beta$  and  $\theta$  depending on  $x$  and  $p$  only through the combination  $z = pb - Gx$ . From the requirement that the effective Hamiltonian for field  $\Phi$  is only  $iv_F \partial_x$  we get

$$\theta(z) = \frac{1}{v_F} \int^z dz \tilde{\mathcal{T}}(z) \quad (6)$$

and a system of differential equations for functions  $\alpha$  and  $\beta$

$$\begin{aligned} iv_F \alpha'_f(z) &= -\mathcal{T}(z) \alpha_f(z) - V \beta_f^*(z) \\ iv_F \beta'_f(z) &= -\mathcal{T}(z) \beta_f(z) + V \alpha_f^*(z). \end{aligned} \quad (7)$$

Note that  $\theta(z + 2\pi) = \theta(z)$  and that  $\alpha_+(z) = \alpha^*(z)$  and  $\beta_+(z) = \beta^*(z)$ , so that it suffices to follow e. g. solutions  $\alpha_+(z), \beta_+(z)$  of the system (7). According to Floquet theory these solutions can be written in the form  $\alpha(z) = A(z) \exp(-iz\delta)$ ;  $\beta(z) = B(z) \exp(iz\delta)$ .  $A$  and  $B$  are periodic with the period  $2\pi$ , and the closer inspection shows that the Floquet exponent  $\delta$  for the system (7) is real for all values of parameters, at least after keeping in  $\mathcal{T}(z)$  only the leading term  $t_1$ .

Once we find  $A$ ,  $B$  and  $\delta$  the wave functions  $\langle x, p | F_k \rangle$  of the states created by  $\Psi^\dagger(x, p)$  are known. The corresponding spectrum is one-dimensional,  $E_k = v_F f(k - k_F)$ . Projection of  $|F_k\rangle$  to the plane wave  $\langle k', p |$  is

$$\begin{aligned} \sum_N \left\{ \mu_k e^{i(N-\delta)pb} \delta[k' - k + G(N-\delta)] \begin{pmatrix} a_N \\ -\hat{b}_N \end{pmatrix} + \right. \\ \left. + \nu_k e^{i(N+\delta)pb} \delta[k' - k + G(N+\delta)] \begin{pmatrix} b_N \\ \hat{a}_N \end{pmatrix} \right\} \quad (8) \end{aligned}$$

Coefficients  $a_N$ ,  $b_N$ ,  $\hat{a}_N$  and  $\hat{b}_N$  are Fourier components of the products  $A \exp(i\theta)$ ,  $B \exp(i\theta)$ ,  $A^* \exp(i\theta)$  and  $B^* \exp(i\theta)$  respectively. Coefficients  $\mu_k$  and  $\nu_k$  are fixed by initial conditions. The expression (8) tells us how the plane wave  $\exp(ikx + pR_\perp)$  is decomposed into discrete states  $N$ . Each state  $N$  is split by  $\delta$  in a way that components with the tilt  $-\delta$  have the statistical weight  $|\mu_k|^2(|a_N|^2 + |\hat{b}_N|^2)$  and the ones with the tilt  $+\delta$  have the weight  $|\nu_k|^2(|b_N|^2 + |\hat{a}_N|^2)$ . Green function  $\langle \Psi(x, p) \Psi^\dagger(x', p) \rangle$  is easily constructed using transformation (5) and knowing that  $\langle \Phi \Phi^\dagger \rangle = (i\omega_n - iv_F f \partial_x)^{-1} = G_{1D}$ .

The Floquet exponent  $\delta$  and the functions  $A$  and  $B$  are calculated using the Hill's theory and the fundamental matrix method [18, 19]. In the present work we limit our calculations to first harmonics in Eq. 4 only, parameterized with  $t_1 = t_b$  and  $t'_1 = t'_b$ . Let us concentrate on the magnetic field dependence of the Floquet exponent  $\delta$  that splits the QNM spectrum as given by Eq. 2. Figure 1(a) shows the energy  $\omega_c \delta$  (in units of  $V$ ) as a function of

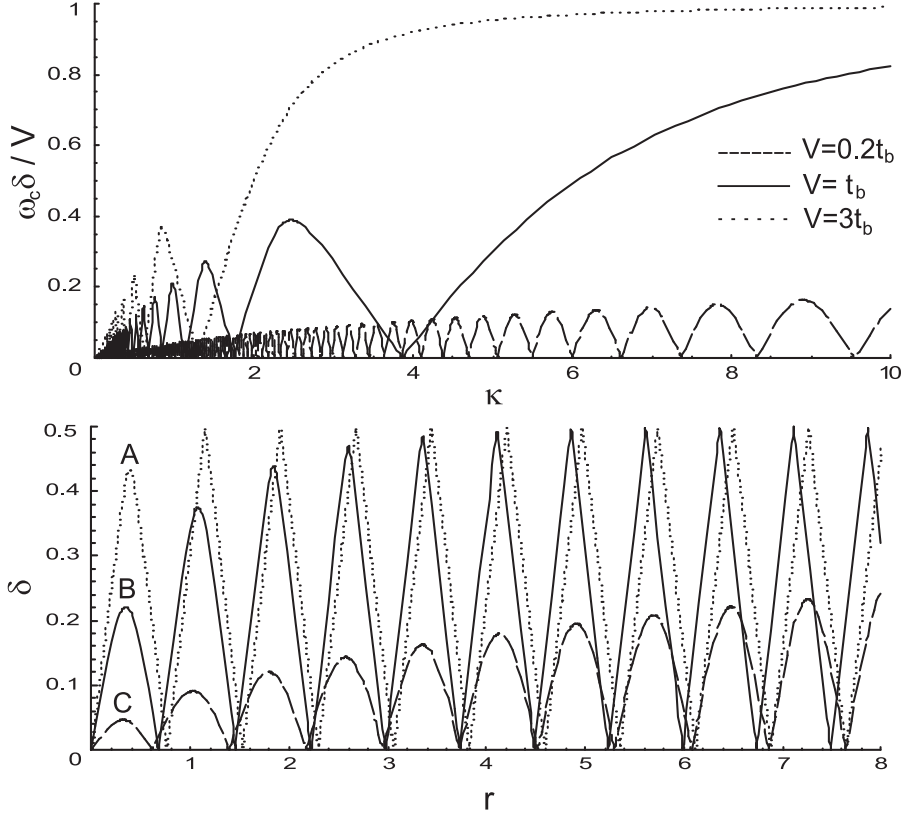


FIG. 1: (a) Energy ratio  $\omega_c \delta / V$  as function of the magnetic breakdown parameter  $\kappa$  for several values of  $V/t_b$ . (b) Dependence of  $\delta$  on  $r$  for  $\theta = 10^\circ$  (A),  $45^\circ$  (B), and  $80^\circ$  (C).

the magnetic breakdown parameter  $\kappa \equiv 2\omega_c t_b / V^2$ , where  $\omega_c = v_F G$  is the cyclotron frequency. In quasi-classical picture  $\kappa$  determines the probability of the over-gap tunnelling  $P = \exp(-\pi/2\kappa)$ . [16] One sees that the crossover from oscillating to saturating behavior does not coincide with the crossover from the weak ( $\kappa < 1$ ) to the strong ( $\kappa > 1$ ) MB. The position of the last zero of  $\delta$  is not universal in  $\kappa$ , but approximately in  $r \equiv [(\gamma V)^2 + t_b^2]^{1/2} / \omega_c$ , where the value of  $\gamma$  is 0.77. Fig. 1(b) shows  $\delta(r)$  for several "polar angles" defined by  $\tan \theta \equiv t_b / \gamma V$ . Oscillations of  $\delta$  are approximately periodic in  $r$  with a period of 0.80. Choosing the parameters  $t_b = 300K$ ,  $v_F = 2 \times 10^5 m/s$ , and  $b = 7.7 \times 10^{-10} m$  we fit RO at 260 Tesla by putting  $V \approx 0.8t_b$ .

Taking the limit of strong magnetic field  $\omega_c / t_b \gg 1$  and of weak anion potential  $V/t_b \ll 1$  we can easily reproduce the 1D spectrum of Osada et al. [15],  $E_k \rightarrow f v_F (k - k_f) \pm \omega_c \delta$  with  $\delta \rightarrow (V/\omega_c) \mathcal{J}_0(4t_b/\omega_c)$ ,  $\mathcal{J}_0$  being the Bessel function. On the other hand the spectrum of Gor'kov and Lebed [16] is reproduced for weak anion potential,  $V/t_b \ll 1$ . [18] The above fit, as well as other insights [20, 21] however strongly suggest that  $V$  in  $(TMTSF)_2ClO_4$  is rather large, i. e. comparable to  $t_b$ .

We proceed with the solution of the interacting problem. Neglecting the absence of a presumably small Umklapp scattering, the effective coupling for SDW is the

forward scattering amplitude  $g_2$ , here simply denoted by  $U$ . We employ the matrix RPA formalism developed in Ref.[12]. The resulting relevant bare susceptibility is  $\chi_1(\mathbf{q}; T) = \frac{1}{2} \{ \chi_{aa} + \chi_{hh} + [(\chi_{aa} - \chi_{hh})^2 + 4(\chi_{ha})^2]^{1/2} \}$ , playing in the Stoner criterion

$$1 - U \chi_1(\mathbf{q}_c, T_c) = 0, \quad (9)$$

$\mathbf{q}_c$  being the wave vector at which  $\chi_1(\mathbf{q})$  has the maximum. The ratio of two SDW order parameters from Eq.(1) is also a function of bare correlators  $\chi_{aa}, \chi_{hh}, \chi_{ah}$  in the  $(a, h)$  basis (see [12]). The bare correlators in the magnetic field are given by

$$\begin{aligned} \chi_{hh} &= \sum_N \left[ |I_{h0}|^2 P_0 + \frac{1}{2} I_{h+}^2 P_+ + \frac{1}{2} I_{h-}^2 P_- \right], \\ \chi_{aa} &= \sum_N \left[ |I_{a0}|^2 P_0 + \frac{1}{2} I_{a+}^2 P_+ + \frac{1}{2} I_{a-}^2 P_- \right], \\ \chi_{ha} &= \sum_N \left[ \Re(I_{h0} I_{a0}^*) P_0 + \frac{1}{2} I_{h+} I_{a+} P_+ - \frac{1}{2} I_{h-} I_{a-} P_- \right], \end{aligned} \quad (10)$$

where  $P_0, P_{\pm}$  stand for  $P(q_{\parallel} - NG, T)$  and  $P[q_{\parallel} - G(N \pm 2\delta), T]$  respectively,  $P(k, T)$  being the familiar 1D Lindhard function at the wave number  $2k_F + k$ .  $P_0$  and  $P_{\pm}$  are the inter-band and the intra-band susceptibilities of

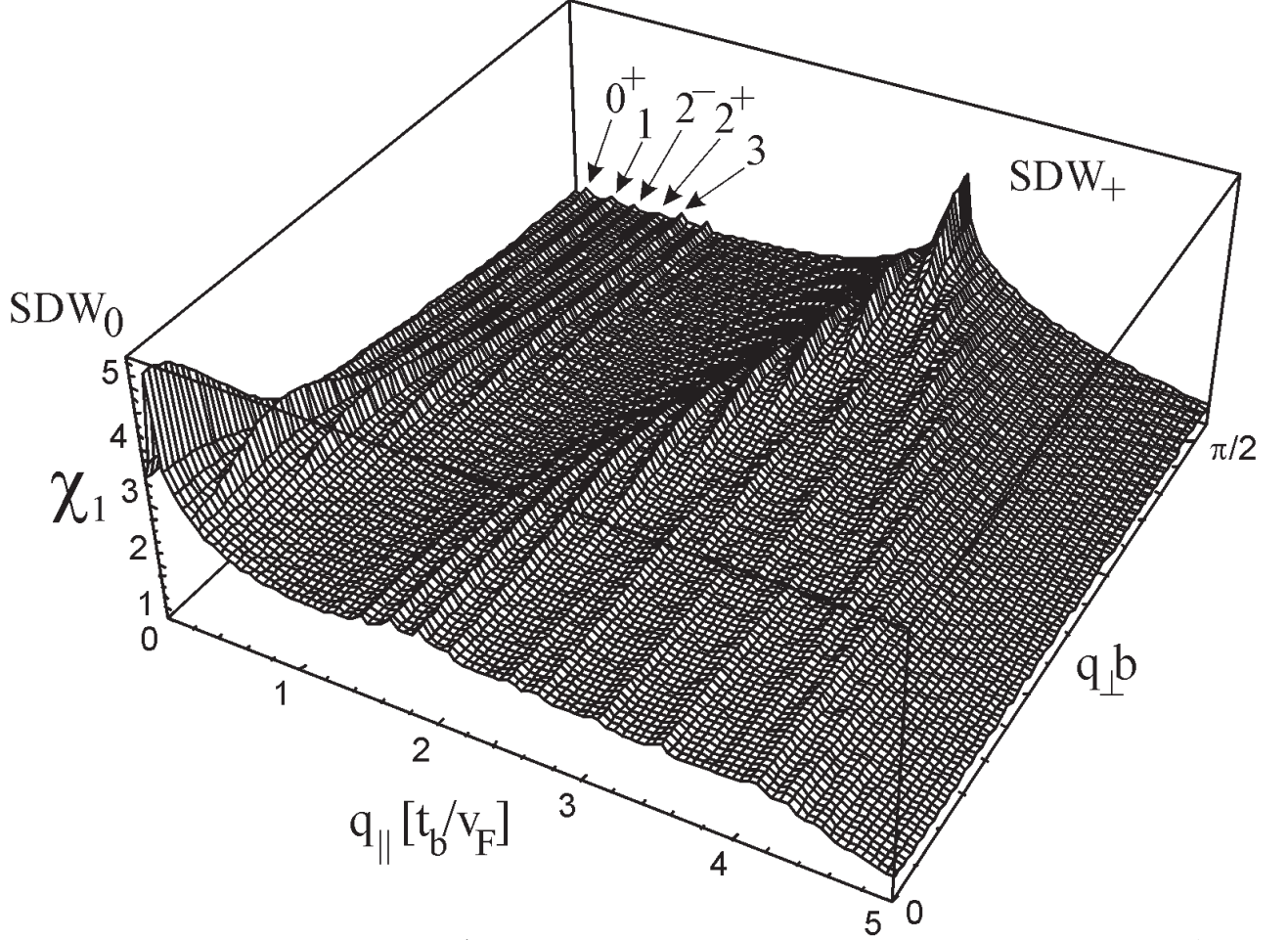


FIG. 2: Susceptibility  $\chi_1$  [in units of  $(2\pi v_F)^{-1}$ ]. Arrows indicate the longitudinal coordinates of the peaks at  $2\delta$  ( $0^+$ ),  $G$  (1),  $2G - 2\delta$  ( $2^-$ ),  $2G + 2\delta$  ( $2^+$ ), and  $3G$  (3). Maximum of  $\chi_1$  corresponds to the phase ( $0^+$ ) for  $\mathbf{q} = (2G, 0)$ .

the  $N$ -th split level in the decomposition (8). The dependence on the transverse momentum is present in the amplitudes  $I(q_\perp, N)$ ,

$$\begin{aligned}
 I_{h0}(q_\perp, N) &= \sum_n (a_n b_{N-n} - \hat{b}_n \hat{a}_{N-n}) e^{i(n-N/2)q_\perp} \\
 I_{h+}(q_\perp, N) &= \sum_n (\hat{a}_n \hat{a}_{N-n} + b_n b_{N-n}) e^{i(n-N/2)q_\perp} \\
 I_{h-}(q_\perp, N) &= \sum_n (a_n a_{N-n} + \hat{b}_n \hat{b}_{N-n}) e^{i(n-N/2)q_\perp} \\
 I_{a0}(q_\perp, N) &= \sum_n (a_n \hat{a}_{N-n} - \hat{b}_n b_{N-n}) e^{i(n-N/2)q_\perp} \\
 I_{a+}(q_\perp, N) &= \sum_n (\hat{a}_n b_{N-n} + b_n \hat{a}_{N-n}) e^{i(n-N/2)q_\perp} \\
 I_{a-}(q_\perp, N) &= \sum_n (a_n \hat{b}_{N-n} + \hat{b}_n a_{N-n}) e^{i(n-N/2)q_\perp}
 \end{aligned} \tag{11}$$

There are two important selection rules for these amplitudes, namely for  $N$  even,  $I_{h0}(N) = I_{a0}(N) = 0$  while for  $N$  odd,  $I_{h\pm}(N) = I_{a\pm}(N) = 0$ . Thus the interband processes contribute only to FISDW phases with odd  $N$

while the intraband processes contribute only to phases with even  $N$ . Consequently only phases with even  $N$  "see" the splitting by  $\delta$ .

The  $\mathbf{q}$ -dependence of the susceptibility  $\chi_1(\mathbf{q})$  for the particular choice of parameters,  $\omega_c = 0.1t_b$ ,  $V = 0.8t_b$ ,  $t'_b/t_b = 0.03$ ,  $T/t_b = 0.001$ , is shown in Fig. 2. The overall envelope assumes the shape present already in the absence of magnetic field [12]. It is now superimposed by a well known characteristic of FISDW susceptibilities [2], logarithmic peaks corresponding to single one-dimensional bubbles  $P(k)$ , weighted by  $p$ -dependent amplitudes as defined by Eqs.(10,11). Qualitatively new feature regarding these peaks is the splitting of peaks with even  $N$  by  $\pm\delta$  around the positions at  $k = NG$ .

According to Eq.(9) at  $T = T_c$  the highest of peaks in Fig. 2 attains the value  $1/U$ . Fig.3 shows the resulting phase diagram for a realistic choice of parameters,  $V = 0.85t_b$ ,  $t'_b = 0.03t_b$  and  $T_c(V = t'_b = 0) = 13K$ . The resulting maximal critical temperature within the present field range is  $T_c^{\max} \approx 1.1K$ . The most obvious characteristic of the obtained phase diagram is the first order transition from  $SDW_0$  to  $SDW_\pm$  at  $B_c \approx 9$  Tesla. Dependence  $T_c(B)$  for  $B < B_c$  is similar to the FISDW cascade

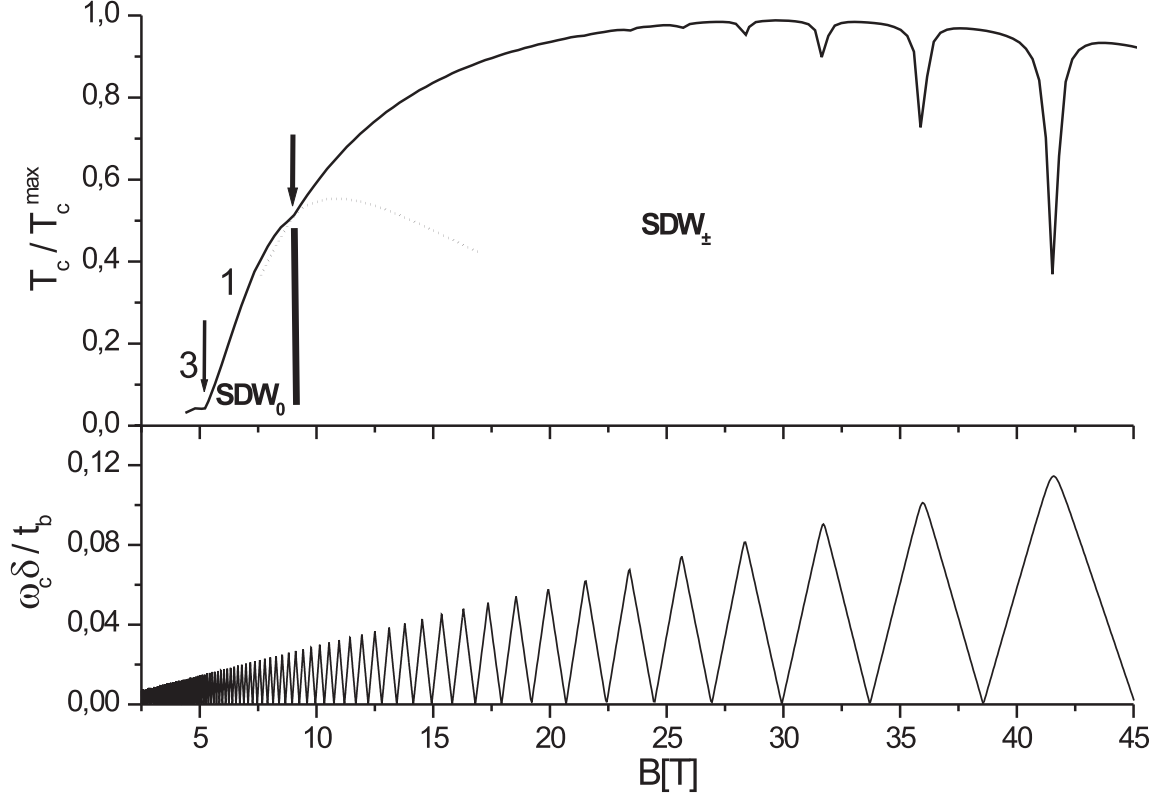


FIG. 3: (a) Phase diagram. (b) Energy ratio  $\omega_c \delta / t_b$  on the same magnetic scale as the phase diagram.

in  $\text{TMTSF}_2\text{PF}_6$ , with the difference that here only odd phases appear because the even ones are suppressed by splitting. For  $B > B_c$  the critical temperature increases towards the highest value  $T_c^{\text{max}}$ . As the magnetic field further increases the critical temperature  $T_c(B)$  starts to oscillate, with the sharp dips corresponding to commensurability condition  $2G\delta = G$  between the Floquet wave number and the magnetic wave number.

Note that the present choice of anion potential  $V = 0.85t_b$  places us in the intermediate regime on scale  $V$  [12] where the response of both  $\text{SDW}_0$  and  $\text{SDW}_\pm$  is suppressed for  $B = 0$ . Hence, being of comparable magnitude the two instabilities compete once they are restored by magnetic field. Both phases in fig.3 are sensitive to  $V$ , general trend being that by increasing  $V$  one decreases  $T_c(\text{SDW}_0)$  and increases  $T_c(\text{SDW}_\pm)$ . The parameter of imperfect nesting in the standard model,  $t'_b$ , here affects only  $\text{SDW}_0$ , while for  $\text{SDW}_\pm$   $t'_b$  plays a role of an effective nearest neighbor hopping. We remind that the effective parameter of imperfect nesting for  $\text{SDW}_\pm$  is a function of  $t_b/V$ , as pointed out in Ref. [12].  $t'_b$  acts on  $\text{SDW}_0$  in a standard way [4], i. e. it fixes the width of the FSDW cascade  $\Delta\omega_c \sim t'_b$  so that by increasing  $t'_b$  one reduces  $T_c(\text{SDW}_0)$  at fixed  $B$ .

The result of the subtle interplay between two scales  $V$  and  $t'_b$  is that the realistic profile of the phase diagram

is possible only within a rather restricted range of the  $(V, t'_b)$  space. By increasing  $V$  or  $t'_b$  by a few percent one reduces  $T_c(\text{SDW}_0)$  below  $T_c(\text{SDW}_\pm)$  in the whole  $B$  domain. On the other hand by decreasing  $V$  by a few percents one gets a hump in  $T_c(\text{SDW}_0)$  on the left of the transition  $\text{SDW}_0 - \text{SDW}_\pm$ .

The rapid oscillations in observable response functions are related to the oscillations of  $\delta$  [16], shown in Fig.3(b). Generally, we expect RO to be visible if two conditions are fulfilled. First, in order to have an over-gap interference one needs a moderate MB parameter,  $\kappa \sim 1$ . Second, one has to be in the oscillating regime on the scale  $r$ , which is equivalent to  $\kappa < \rho(V/t_b) \equiv 2(V/t_b)^{-2} \sqrt{(\gamma V/t_b)^2 + 1}$ . Fig.3(b) shows how the energy tilt  $\omega_c \delta$  varies in various parts of the phase diagram. At 30 Tesla we have  $\kappa \sim 0.5$  and  $\rho(0.85) \approx 3.3$ , so that both conditions are fulfilled. The effect is expected to be even stronger for higher fields because  $\kappa$  then increases.

The maximal value of the critical temperature in Fig.3,  $T_c^{\text{max}} \approx 1.1\text{K}$ , is considerably smaller than the experimental value of 5.5K. In this respect we note that  $T_c^{\text{max}}$  is essentially model dependent quantity, i. e. that the Hamiltonian (3) represents a *minimal* model for understanding the interplay between two SDW phases in the magnetic field. Namely, recent experiments [21] suggest that the anion ordering in  $\text{TMTSF}_2\text{ClO}_4$  induces

also, beside a strong dimerizing potential  $V$ , rather large changes in other band parameters.

The present treatment also does not include the quantitative analysis of the splitting of degeneracy of two intraband phases,  $SDW_+$  and  $SDW_-$ . Physically the degeneracy is lifted because the realistic tight-binding dispersion along the chain is not strictly linear. Consequently the dominant instability will be that of  $SDW_-$ , as discussed in Ref.[12]. Similar conclusions were obtained also by numerical calculations [22], but without taking into account the two component aspect of the order parameter (1). The second critical temperature can be calculated within Landau theory as in Ref.[13], and by taking the nonlinearity of the band dispersion into

account. The subphases of the high-field phase correspond to  $SDW_+$  phases within  $SDW_-$ , each one nesting its own pair of Fermi sheets. Such scenario is impossible for  $SDW_0$  since it proceeds through nesting of all four sheets at the *single* critical temperature.

In conclusion, we have solved exactly the one-particle problem of dimerized Q1D band of electrons in magnetic field. Observables contain characteristic periodicity in  $1/B$ , consistent with 260 Tesla oscillations in normal and SDW phases of  $(TMTSF)_2ClO_4$ . Using matrix RPA for SDW susceptibility we reproduce the first-order transition between two types of FSDW ordering, as well as the overall profile of the experimental phase diagram.

- 
- [1] T. Ishiguro, K. Yamaji, and G. Saito, Organic Superconductors IIe, (Springer-Verlag, Berlin, 1998).
  - [2] P. M. Chaikin, J. Phys. I (France) **6**, 1875 (1996); P. Lederer *ibid.* **6**, 1899 (1996); V. M. Yakovenko and H. S. Goan *ibid.* **6**, 1917 (1996).
  - [3] N. Biškup *et al.*, Phys. Rev. B **60**, 15005 (1999).
  - [4] For historical references and recent developments of the quantum nesting model, see A. G. Lebed, Phys. Rev. Lett. **88**, 177001 (2002).
  - [5] J. S. Qualls *et al.*, Phys. Rev. B **62**, 12680 (2000).
  - [6] N. Matsunaga *et al.*, Phys. Rev. B **62**, 8611 (2000); cond-mat/0206010.
  - [7] S. K. McKernan *et al.*, Phys. Rev. Lett. **75**, 1630 (1995).
  - [8] O.-H. Chung *et al.*, Phys. Rev. B **61**, 11 649 (2000).
  - [9] W. Kang *et al.*, Synthetic Metals **120**, 1073 (2001).
  - [10] A. Bjeliš and K. Maki, Phys. Rev. B **45**, 12887 (1992).
  - [11] S. Uji *et al.*, Solid State Commun. **103**, 387 (1997).
  - [12] D. Zanchi and A. Bjeliš, Europhys. Lett. **56**, 596 (2001).
  - [13] K. Sengupta and N. Dupuis, Phys. Rev. B **65**, 035108 (2002).
  - [14] R. W. Stark and C. B. Friedberg, J. Low Temp. Phys. **14**, 111 (1974).
  - [15] T. Osada *et al.*, Phys. Rev. Lett. **69**, 1117 (1992).
  - [16] L. P. Gor'kov and A. G. Lebed, Phys. Rev. B **51**, 3285 (1995); *ibid.* 1362.
  - [17] K. Yamaji, J. Phys. Soc. Jpn. **51**, 2787 (1982).
  - [18] D. Radić, A. Bjeliš and D. Zanchi, to be published.
  - [19] S. L. Ross, Differential Equations, 3rd edition (John Wiley & Sons, New York, 1984). pp. 505-521; E. L. Ince, Ordinary Differential Equations (Dover Publ., 1956) pp. 384,503,507; E. Kamke, Differentialgleichungen (Akademische Verlag. Becker & Erler Kom.-Ges., Leipzig, 1942).
  - [20] H. Yoshino *et al.*, J. Phys. Soc. Jpn. **68**, 3142 (1999).
  - [21] D. Le Pévelén *et al.*, Eur. Phys. J. B **19**, 363 (2001).
  - [22] K. Kishigi, J. Phys. Soc. Jpn. **67**, 3825 (1998).